XLVI CILAMCE
VITÓRIA - ES - BRAZIL - 2025
XLVI IBERO-LATIN AMERICAN CONGRESS ON COMPUTATIONAL METHODS IN ENGINEERING

Parametric Stability Analysis of Thin-Walled Polygonal Tubular Members Using the Finite Strip Method

Matheus Ítalo de A. Alves[1], Eduardo de Miranda Batista[1], Michèle Schubert Pfeil[1]

[1]*COPPE, Civil Engineering Program, Federal University of Rio de Janeiro. Brazil*
Centro de Tecnologia, Bloco I, Sala I216, Ilha do Fundão, 21945-909, Rio de Janeiro/RJ, Brazil
matheus.alves@coc.ufrj.br, batista@coc.ufrj.br, mpfeil@coc.ufrj.br

Abstract. This paper presents a parametric study on the stability of steel thin-walled polygonal tubular sections, aiming at typical applications in telecommunication towers. The geometries cover variations in diameter (D), thickness (t), and number of sides (n, from 6 to 20), synthesized through the parameters D/t and relative slenderness ratios. The elastic critical bending moments and axial loads (M_{cr}, N_{cr}) were obtained using the Finite Strip Method (FSM) through the software FStr Computer Application, with modal identification performed via signature curves. A predominance of local buckling was observed across the sample, while distortional buckling occurred in only two cross-sections under axial compression, precisely those with the lowest D/t ratios. In terms of overall trends, increasing D/t led to reductions in N_{cr} and M_{cr}. Normalization by plastic reference quantities (N_{cr}/N_y, M_{cr}/M_y) and the use of relative slenderness parameters substantially reduced data dispersion and produced consistent results, according with classical design formulations. As the main contribution, this work provides and discusses the key trends related to the influence of geometric parameters on the stability of polygonal tubular sections under compression and bending. Finally, comprehensive normalized results on the structural performance of cold-formed, thin-walled steel polygonal members are presented, with a focus on engineering applications for posts supporting telecommunication antennas.

Keywords: Thin-walled steel structure, cold-formed steel, polygonal tubular sections, buckling analysis.

1 Introduction

Steel tubular members are widely used in various structural applications due to their high mechanical efficiency, strength, and versatility. This solution is commonly used in lighting poles, monopole and monotubular towers for telecommunication and power transmission, as well as in large wind and lighting towers, where they provide safe support, durability, and good aesthetic performance. Polygonal cross-sections, in particular, offer improved stiffness and spatial efficiency, since their narrower flat sides, compared to rectangular sections with the same perimeter, resulting in more efficient walls and a more uniform stress distribution [1,2]. Despite these advantages, the use of thin-walled polygonal tubes in tall towers introduces specific design challenges, mainly due to their high slenderness and susceptibility to local and distortional buckling [3].

This work is part of the ongoing master's dissertation of the first author, dedicated to the study of thin-walled steel tubular structures with polygonal cross-sections, focusing on optimized design of posts for telecommunication support antennas. The overall research project comprises four stages: (i) a parametric study of 69 polygonal profiles using the Finite Strip Method (FSM) with the FStr software [4]; (ii) the design and verification of the corresponding towers according to NBR 14762 [5], identifying promising cross-sections for 40 m towers; (iii) the numerical modeling of a representative tower (40 m, 20-sided) under static wind loading according to NBR 6123 [6]; and (iv) a dynamic analysis (modal evaluation and frequency domain) with verification of the Ultimate and Serviceability Limit States (ULS and SLS).

The scope of this paper is limited to the stability analyses of thin-walled polygonal cross-sections derived from stage (i). The objective is to identify local and global buckling trends as functions of geometric parameters

and synthesis relations, providing input for preliminary design, design calibration, and the selection of suitable cross-sections for the mentioned applications. The tower modeling and wind action stages, although part of the broader research, are not addressed in this paper.

2 Selection of Cross-Sections

The selection of the 69 polygonal cross-sections was based on the geometric criteria established by Gonçalves and Camotim [3], in which the adopted parameter ranges and increments were defined to represent feasible configurations for structural applications, ensuring that the generated numerical models are both representative and practically relevant. Diameters were considered within the range of 1.0 to 2.0 meters, with increments of 0.2 meters (1.0, 1.2, 1.4, 1.6, 1.8, and 2.0 meters), where D represents the outer diameter corresponding to the circumscribed circle of the polygonal section. The number of polygon sides varied from 6 to 20, considering only even values, since sections with an odd number of sides exhibit asymmetric behavior in which adjacent walls deform in the same direction, breaking the alternating buckling pattern and reducing the effective stiffness of the section [7]. This allowed the analysis of the transition between geometries approaching a circular section (large number of sides) and those with fewer sides, which represent more faceted shapes. The wall thicknesses were selected based on commercially available thin steel sheets, comprising the values of 2.00, 2.25, 2.65, 3.00, 3.35, 3.75, 4.25, 4.75, and 6.35 mm.

A strategic approach was adopted, in which the selection of models began with a broad parametric study varying diameter, thickness, and number of sides. Based on the results obtained in this initial phase, progressive refinements were conducted, gradually reducing the sample space as structural behavior patterns were identified.

3 Buckling Analysis with the Finite Strip Method

The calculation of the design resistances for bending (M_{Rd}) and axial compression ($N_{c,Rd}$), according to the criteria established in the Brazilian code NBR 14762, requires prior knowledge of the critical loads associated with local and distortional buckling modes. Therefore, it is necessary to determine the critical bending moments for local (M_{crL}) and distortional (M_{crD}) buckling modes, as well as the corresponding critical axial loads (N_{crL} and N_{crD}) [8]. The determination of these critical values is essential for the proper design of thin-walled polygonal tubular profiles, ensuring that strength verifications are performed considering the most significant instability modes for each analyzed geometric configuration.

To determine these values, the computational tool FStr was employed. This software was specifically developed for the analysis of thin-walled sections, using the Finite Strip Method (FSM) originally formulated by Cheung [9]. While the Finite Element Method (FEM) employs polynomial shape functions in all directions, the FSM combines polynomial functions in the transverse direction and trigonometric functions in the longitudinal direction, satisfying the boundary conditions for small displacements and allowing a simplified yet accurate solution to the buckling problem.

The identification of local (short length), distortional (medium length), and global (long length) buckling modes was carried out through the interpretation of signature curves, which map the buckling solutions obtained in FStr as a function of the member length L, for simply supported profiles subjected to constant internal forces along the span, as illustrated in Figure 1. The half-wavelength range analyzed varied from 0.1 m to 100 m, adopting the steel Young modulus and Poisson ratio, respectively E = 200 GPa and ν = 0.3, and simply supported end conditions with free rotations and warping. The half-wavelength interval of 0.1 m to 100 m was adopted solely as a computational analysis domain for the generation of signature curves within the FStr model. This range was chosen to cover the expected order of magnitude of the elastic buckling solutions relevant to the type of structures, considered in the first author's MSc dissertation, particularly for polygonal tubular towers up to 40 m height.

Although not presented in this paper, it is worth noting that the design resistances were successfully evaluated using the Effective Section Method (ESM) [10], prescribed in NBR 14762, based on the effective geometric properties of the analyzed thin-walled polygonal cross-sections, for members subjected to axial compression and bending.

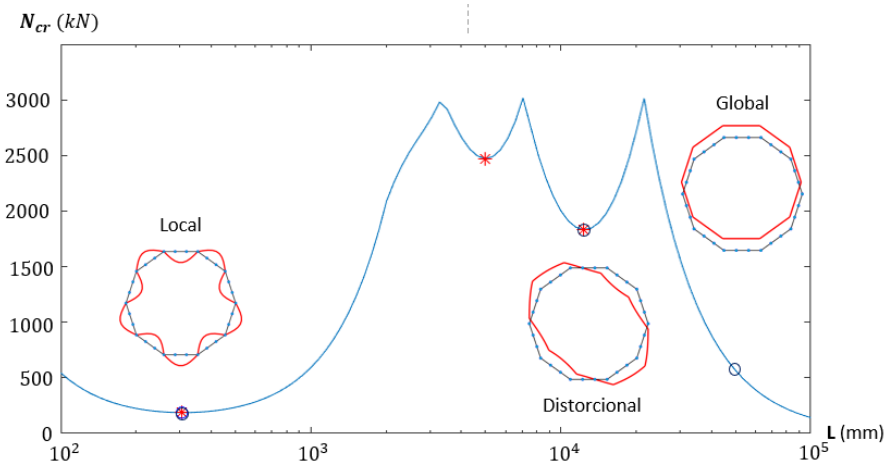


Figure 1. FStr software results of the signature curve for axial loading (N_{cr} *vs.* L) of the tubular profile (n =10 sides, D = 1m, and t = 2mm).

4 Geometric Parametric Study

The geometric parametric study aimed to systematically investigate the influence of the main geometric variables (number of sides, outer diameter, and wall thickness) of the structural behavior of thin-walled polygonal steel tubular profiles. The adopted profiles were analyzed using the Finite Strip Method (FSM) implemented in the FStr software, in order to determine the critical axial loads and bending moments associated with local and distortional buckling. Figure 2 illustrates these behaviors through overlapped signature curves corresponding to cross-section groups where a single geometric parameter was varied independently.

4.1 Influence of the Number of Sides

The analyses showed that the number of sides has a direct influence on structural stability. Profiles with fewer sides exhibit more pronounced flat regions, making them more vulnerable to local buckling. Conversely, as the number of sides increases, the behavior of the polygonal section approaches that of a circular section (axisymmetric circular shell member), leading to higher critical loads and lower effective local slenderness. When isolating sets of profiles with the same diameter and thickness, it became evident that increasing the number of sides causes vertical upward shifts in the signature curves, raising the critical load levels over almost the entire range of analyzed half-wavelengths. This critical wavelength also shifted toward smaller values, since the critical half-wavelength for local buckling is proportional to the wall width, which decreases as the number of sides increases.

4.2 Influence of Diameter Variation

An increase in diameter led to a higher moment of inertia and greater torsional stiffness, improving structural performance under bending and lateral–torsional buckling. On the other hand, this increase also raised the global slenderness (relative to length and radius of gyration), which negatively affected the compressive resistance at certain instability lengths. Consequently, a reduction was observed in the minimum values of the critical load N_{crL}, accompanied by an increase in the corresponding critical half-wavelength L. The analysis for bending moment, however, exhibited a distinct behavior. As the diameter increased for profiles with the same number of sides and thickness, the minimum values of the critical moment M_{crL} remained practically constant among the different profiles, with variation occurring only in the critical half-wavelength, which shifted to higher values as the diameter increased. The constancy of M_{crL} occurs because, in the analyzed geometries, the critical mode is local: the instability develops in the wall itself rather than in the structure as a whole. Since the wall thickness remained constant and the increase in panel width was modest (diameters ranging from 1 to 2 m), the critical capacity varied little; the only significant change was the critical half-wavelength, which increased with diameter. Therefore, the diameter has a greater influence on global instability under compression than on local buckling under bending.

4.3 Influence of Wall Thickness

Regarding the variation of wall thickness between 2.0 mm and 6.35 mm for profiles with the same number of sides and diameter, a direct positive effect was observed: the increase in thickness raised both the critical loads and moments for buckling without significantly altering the critical half-wavelength. This behavior is consistent with the fact that, in local buckling modes, the most sensitive parameter is the local stiffness of the wall, while the characteristic wavelength of instability remains nearly constant when the panel width and boundary conditions do not vary. The results demonstrate that increasing wall thickness enhances the structural performance under both axial compression and bending.

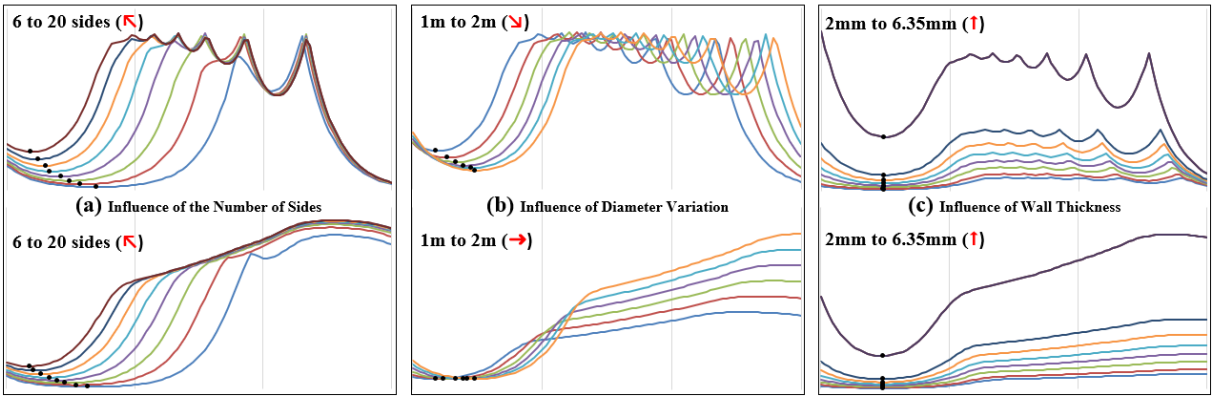


Figure 2. Simplified signature-curve plots showing the influence of (a) number of sides, (b) diameter, and (c) wall thickness. Upper plots refer to N_{cr} *vs* L and lower plots to M_{cr} *vs* L.

4.4 Influence of Wall Slenderness and Relative Slenderness

By using dimensionless parameters, it was possible to interpret the effects of geometric variations on structural performance in a unified way, enabling comparisons and generalizations among different profiles. The wall slenderness (λ) is defined as the ratio between the width of the compressed plate and its thickness (b/t), and in tubular profiles it is commonly expressed as D/t, Where D represents the equivalent outer diameter. This geometric parameter directly reflects the wall's susceptibility to local buckling: the higher the slenderness, the greater the tendency toward premature instability due to local stiffness loss. In addition to the pure geometric slenderness (D/t), the parametric analysis was complemented by the evaluation of the dimensionless relative slenderness parameters $\lambda_{rel,N}$ for axial compression and $\lambda_{rel,M}$ for bending moment. These parameters were formulated according to the principles of the Direct Strength Method (DSM) [11], as adopted in ABNT NBR 14762. For members subjected to axial compression, the local relative slenderness is defined in Equation 1.

$$\lambda_{rel,N} = \sqrt{\frac{N_y}{N_{cr}}} \tag{1}$$

With $N_y = Af_y$ as the plastic axial yield load of the section, and N_{cr} as previously presented, the critical buckling load obtained from elastic buckling analysis. Similarly, for members subjected to bending, the relative slenderness is defined in Equation 2, with $M_y = Wf_y$ as the bending moment corresponding to the onset of yielding, and M_{cr} as the critical buckling moment obtained from the elastic buckling analysis.

$$\lambda_{rel,M} = \sqrt{\frac{M_y}{M_{cr}}} \tag{2}$$

These parameters allow the cross-section classification from the elasto-plastic behavior ($M_{cr}/M_y > 1$ or $N_{cr}/N_y > 1$), to the elastic buckling behavior with premature local or distortional instability ($M_{cr}/M_y < 1$ or $N_{cr}/N_y < 1$). This is a widely employed classification method for both theoretical approaches and structural design criteria from codes, as the Brazilian one NBR 14762. To provide a comprehensive overview of the structural behavior of the 69 analyzed profiles based on these parameters, Figure 3 shows the variation of the critical axial buckling load N_{cr} as a function of the D/t ratio. Although some data dispersion is observed due to geometric diversity of the sections, a clear trend can be identified: the critical load decreases as this parameter increases, indicating that thinner-walled sections (with higher wall slenderness) are less resistant to local buckling. The same behavior is observed for the critical buckling moment, as shown in Figure 4.

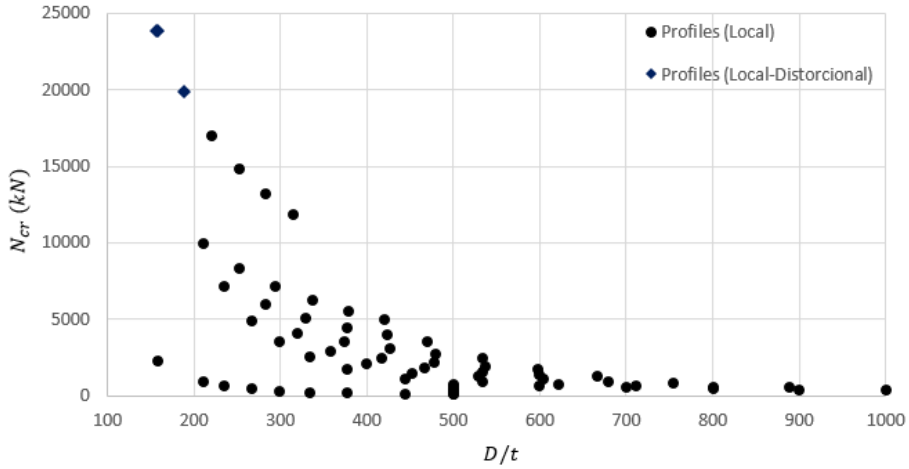


Figure 3. Dispersion of the critical axial buckling load values (N_{cr}) as a function of wall slenderness (D/t) for the 69 analyzed profiles.

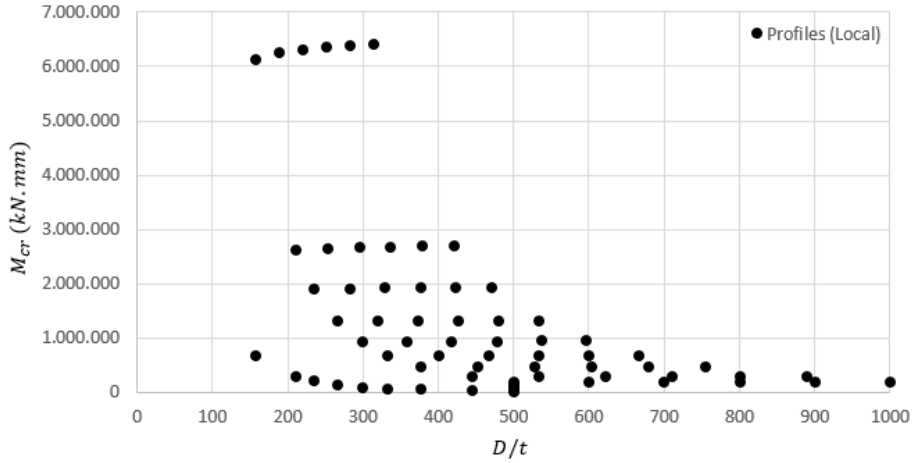


Figure 4. Dispersion of the critical buckling moment values (M_{cr}) as a function of wall slenderness (D/t) for the 69 analyzed profiles.

Regarding the classification of the buckling modes, a comparison was established based on the results obtained with the classification proposed by Martins *et al.* [12], developed using the Generalized Beam Theory (GBT). According to that study, for the ratio between the diameter of the circumscribed polygonal section and the plate thickness (*D/t*): (i) values lower than 140 correspond to distortional buckling, (ii) values between 140 and 240 indicate local–distortional interaction modes, and (iii) values greater than 240 correspond to local buckling. In that work, however, the modulus of elasticity of steel was taken as 210 GPa, instead of 200 GPa of the present study, and the modal classification was determined through GBT, instead of the FSM. In the present study, the buckling modes were identified according to the *D/t* ranges defined in Table 1, derived from the results of the analyses performed with the FStr software. These intervals were established through visual classification based on elastic stability theory, as previously explained and exemplified in Figure 5. Among the analyzed profiles, 67 exhibited local buckling, while only two (both under axial compression) showed distortional buckling contribution.

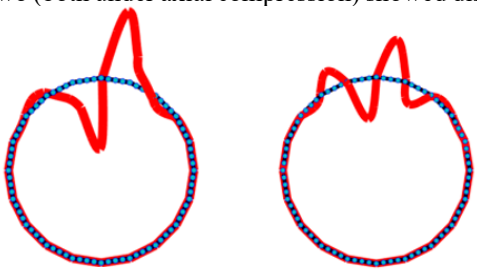


Figure 5. Buckling mode shapes for 20-sided sections under bending loading: (a) local–distortional (D= 1000 mm, t = 6.35 mm, and D/t = 157) and (b) local (D= 1400 mm, t = 6.35 mm, and D/t = 220)

Table 1. Classification of the buckling modes based on the D/t parameter.

(MARTINS *et al.*, 2021)		The present study using the FStr software.	
Range	Buckling mode	Range	Buckling mode
$D/\mathrm{t} < 140$	Distorcional	-	-
$140 < D/\mathrm{t} < 240$	Local-Distorcional	$D/\mathrm{t} < 190$	Local-Distorcional
$D/\mathrm{t} > 240$	Local	$D/\mathrm{t} > 190$	Local

Complementarily, normalization plots of the buckling analysis results with respect to the reference plastic loads of the section were generated for both axial compression (Figure 6) and bending moment (Figure 7). In these figures, the loading ratios N_{cr}/N_y and M_{cr}/M_y are presented as functions of the respective relative slenderness parameters $\lambda_{rel,N}$ and $\lambda_{rel,M}$. The red dashed line represents the conventional limit separating the plastic regime (above 1.0) from the elastic regime (below 1.0). The blue diamond markers (as also used in Figure 3) correspond to the profiles in which distortional buckling contribution was observed, namely: (i) the 20-sided section with D = 1.0 m and t = 6.35 mm, and (ii) the section with similar geometry but D = 1.2 m. The buckling analysis data shows that the vast majority of profiles operate within the elastic regime, especially for relative slenderness values, $\lambda_{rel,N}$ and $\lambda_{rel,M}$, greater than 1.0. As the relative slenderness displays $\lambda_{rel,N}$ and $\lambda_{rel,M}$ lower than 1.0, the critical loading ratios exceed unity, indicating the possibility of yielding development prior to instability.

These relationships are fundamental for the design of members subjected to compression and bending according to ABNT NBR 14762, in which the relative slenderness is directly employed as the decisive parameter for determining member resistance. When the buckling parameters are normalized with respect to the corresponding plastic loads and moments, the data results are well organized, allowing consistent structural interpretation, as shown in Figures 6 and 7. This approach allowed the identification of a clear trend, similar to the well-established design procedures found in standards, such as the Direct Strength Method (DSM) and the Effective Section Method (ESM).

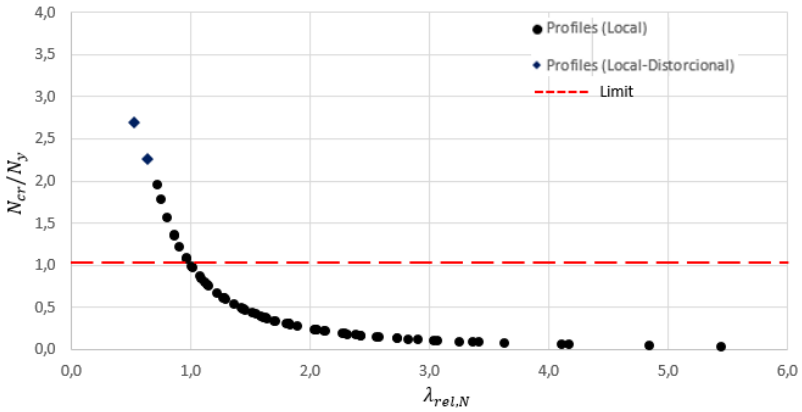


Figure 6. Relationship between the normalized critical axial buckling load and the relative slenderness in compression

5 Conclusions

The parametric buckling analysis of rationally defined 69 geometries of thin-walled polygonal tubular sections using the Finite Strip Method (FSM) revealed a predominance of local buckling, with secondary participation of the distortional buckling, which was observed only in two profiles: (i) n = 20, D = 1.0 m, t = 6.35 mm, and (ii) n = 20, D = 1.2 m, t = 6.35 mm — precisely those with the lowest D/t ratios within the dataset. A monotonic behavior was also observed: increasing *D/t* led to systematic reductions in N_{cr} and M_{cr}, reflecting the greater vulnerability of thinner walls to local instability mechanisms. The influence of the number of sides n was more pronounced in sections with lower D/t ratios, becoming marginal for higher wall slenderness values.

The presented results refer to elastic buckling critical values obtained through FSM, not accounting for manufacturing effects (*e.g.* round or sharp corners). Nevertheless, from a synthesis and application standpoint, the modal identification of buckling, the normalized curves, and the parametric organization of results provide behavioral trends consistent with established design practices, reducing data dispersion and enabling consistent comparative interpretations among cross-section geometric families.

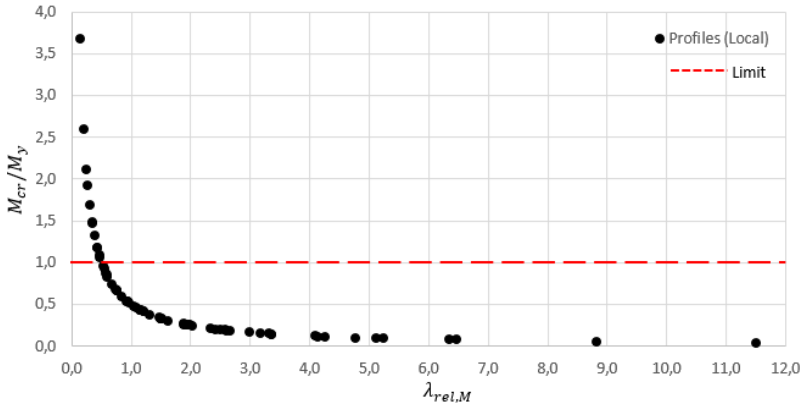


Figure 7. Relationship between the normalized critical buckling moment and the relative slenderness in bending

The identified relationships also support the calibration of design formulations and the development of dimensionless charts for preliminary sizing of polygonal tubular sections, improving the link between numerical predictions and practical design. Furthermore, future studies should incorporate initial geometric imperfections and residual stresses to refine the correlation between elastic buckling predictions and the behavior of such thin-walled sections. These findings support practical guidelines for preliminary design, suggesting the avoidance of high D/t ranges when local instability control is critical, the adoption of a greater number of sides especially for low D/t ratios, and the explicit verification of potential distortional instability before assuming local dominance at low D/t values. Attention should also be given to the plasticity and yielding limits of the sections. Altogether, these synthesized results offer an objective basis for the initial selection of cross-sections in typical applications of towers and masts, which must be complimented with the member design computation, considering both static and wind dynamic assumptions, as included in the final version of the master of science dissertation of the first author (to be concluded in the next few months).

References

[1] H. Fang, T.-M. Chan, and B. Young, "Material properties and residual stresses of octagonal high-strength steel hollow sections," *Journal of Constructional Steel Research*, vol. 184, pp. 479–490, 2018. DOI: 10.1016/j.jcsr.2018.06.007.
[2] J. Chen, H. Liu, and T.-M. Chan, "Material properties and residual stresses of cold-formed octagonal hollow sections," *Journal of Constructional Steel Research*, vol. 170, 2020. DOI: 10.1016/j.jcsr.2020.106078.
[3] R. Gonçalves and D. Camotim, "On the behaviour of thin-walled steel regular polygonal tubular members," *Thin-Walled Structures*, vol. 62, pp. 191–205, 2013. DOI: 10.1016/j.tws.2012.08.006.
[4] J. A. de Lazzari and E. de M. Batista, "Finite strip method computer application for buckling analysis of thin-walled structures with arbitrary cross-sections," *REM – International Engineering Journal*, vol. 74, no. 3, pp. 337–344, 2021.
[5] ABNT – Associação Brasileira de Normas Técnicas, *NBR 14762: Design of steel and composite steel–concrete structures for buildings*, Rio de Janeiro, 2010.
[6] ABNT – Associação Brasileira de Normas Técnicas, *NBR 6123: Wind loads on buildings*, Rio de Janeiro, 2023.
[7] W. Wittrick and P. Curzon, "Local buckling of long polygonal tubes in combined compression and torsion," *International Journal of Mechanical Sciences*, vol. 10, no. 10, pp. 849–857, 1968.
[8] E. de M. Batista, J. A. de Lazzari, G. Y. Matsubara, and M. Pfeil, "Structural dynamic and buckling behaviour of steel cold-formed polygonal conic pole for antennas support," *Civil Engineering Design*, vol. 5, no. 6, pp. 777–789, 2023. DOI: 10.1002/cepa.1740.
[9] Y. K. Cheung, *Finite Strip Methods in Structural Analysis*, Oxford: Pergamon Press, 1976.
[10] E. de M. Batista, "Effective section method: A general direct method for the design of steel cold-formed members under local–global buckling interaction," *Thin-Walled Structures*, vol. 48, nos. 4–5, pp. 345–356, 2010. DOI: 10.1016/j.tws.2010.01.009.
[11] B. W. Schafer and T. Peköz, "Direct strength prediction of cold-formed steel members using numerical elastic buckling solutions," in *Proc. 14th Int. Specialty Conf. on Cold-Formed Steel Structures*, St. Louis, USA, Oct. 15–16, 1998.
[12] A. D. Martins, R. Gonçalves, and D. Camotim, "Post-buckling behaviour of thin-walled regular polygonal tubes subjected to bending," *Thin-Walled Structures*, vol. 166, 2021. DOI: 10.1016/j.tws.2021.107994.